Research Square

Preprints are preliminary reports that have not undergone peer review.
They should not be considered conclusive, used to inform clinical practice,
or referenced by the media as validated information.

The Price of Non-Hermiticity: Exact Stability, Dissipation, and Isolation Bounds for Passive Nonreciprocal Electrical Networks

H.-Y. Liu

3353363748@qq.com

chongqing https://orcid.org/0009-0005-0098-8535

jiangjuaxin

chongqing https://orcid.org/0009-0009-0010-1278

Research Article

Keywords: circuit synthesis, non-Hermitian systems, nonreciprocal circuits, positive-real functions, skin e˙ect, topolectrical circuits

Posted Date: November 9th, 2026

DOI: https://doi.org/10.21203/rs.3.rs-11639667/v1

License: This work is licensed under a Creative Commons Attribution 4.0 International License.
Read Full License

Additional Declarations: The authors declare no competing interests.

The Price of Non-Hermiticity: Exact Stability, Dissipation, and Isolation Bounds for Passive Nonreciprocal Electrical Networks

Haoyi Liu[a,*], Jiaxin Jiang[a]

[a] *Chongqing Institute of Engineering, Chongqing, China*

Abstract

Electrical circuits realize non-Hermitian tight-binding models node by node, but which of them a circuit can actually realize, and at what cost, has not been made quantitative. This paper casts circuit realizability as an inverse problem over three layers—an admissible network class, a frequency-window fingerprint, and resource functionals (component count, dissipation, bandwidth, stability margin, isolation, and throughput)—and solves its one-dimensional instance exactly. Positive-real theory separates the passivity gap from the stability gap: the stability threshold of a nonreciprocal chain is a surface-state value strictly smaller than the usually quoted bulk band edge, and it vanishes for the conservative split. Skin localization in a passive circuit exists but is not free: a passive modulus-changing bond must dissipate a minimum conductance, and isolation is an exact identity that survives arbitrary bond disorder. A complete, tabletop-ready experimental design in the audio band is provided; all closed forms are validated numerically, and component values are specified.

Keywords: circuit synthesis, non-Hermitian systems, nonreciprocal circuits, positive-real functions, skin effect, topolectrical circuits

*Corresponding author

Email addresses: liuhaoyi@cqie.edu.cn (Haoyi Liu), jiangjiaxin@cqie.edu.cn (Jiaxin Jiang)

1. Introduction

The non-Hermitian skin effect (NHSE) [1, 2]—the exponential accumulation of eigenmodes at a boundary under open boundary conditions—together with non-Bloch band theory and point-gap topology has reshaped our understanding of boundary phenomena in open and dissipative systems. Electrical circuits (topolectrical circuits) [3, 4, 5, 6, 7] have emerged as the most flexible experimental platform, because a broad class of non-Hermitian tight-binding matrices can be realized node by node with operational amplifiers, gyrators, and negative-impedance converters (NICs) [8, 9], and measured directly with an oscilloscope.

This flexibility, however, obscures a question that the circuit platform is uniquely positioned to answer: what are the realizability limits themselves? Optical and acoustic implementations fix a physical substrate whose parameters are constrained by material dispersion and fabrication; a circuit does not. A circuit asks the designer to pay for every non-Hermitian feature—in components, in dissipated power, in stability margin, and in bandwidth. This paper derives, in closed form, the prices that a nonreciprocal electrical network must pay—in component count, dissipation, stability margin, and bandwidth—for a prescribed non-Hermitian behavior at its ports. Three results are new: the stability threshold of a nonreciprocal chain is a surface-state eigenvalue strictly below the usually quoted bulk band edge; a passive modulus-changing bond must dissipate at least $2\hat{g}\sinh|\alpha|$; and the end-to-end isolation is an exact identity that survives arbitrary bond disorder.

The organizing idea is that *existence is cheap—classical synthesis theorems guarantee it—and the physics lives in the design cost map.* A rational positive-real node admittance can be synthesized by Brune–Youla–Tissi theory [10, 11, 12] into a passive network with gyrators, and active elements remove the remaining constraint up to a margin; what is not free is the number of nonreciprocal components, the dissipation, the bandwidth, and the stability margin that a given non-Hermitian fingerprint costs. We therefore cast realizability as an inverse problem over three layers, and solve its one-dimensional instance exactly. Every bound below is simultaneously a class-wide lower bound and, in the cases marked *sharp*, an attained value.

The contributions are as follows.

(i) The stability threshold of a nonreciprocal chain is a *surface-state* eigenvalue, strictly smaller than the commonly used bulk band edge, and it vanishes for the conservative split (Section 4).

(ii) A passive modulus-changing bond must dissipate at least $2\hat{g}\sinh|\alpha|$, with a closed-form dissipation–bandwidth tradeoff $W = 2D\,\mathrm{sech}\,\alpha$ (Section 5).

(iii) End-to-end isolation is an exact identity, $|S_{21}/S_{12}| = e^{2\alpha(N-1)}$, surviving arbitrary bond disorder and depending only on the fingerprint $\{\alpha_e\}$ (Section 8).

(iv) Port-visible gain requires negative conductance, with a margin cost that vanishes as α^2 in the weak-skin limit (Section 8).

(v) A complete, tabletop-ready experimental design in the audio band, with component values and falsifiable predictions (Section 10).

Complete proofs are given in Appendices A–G; the disorder stability and throughput functionals (Appendix H), the joint-passivity semidefinite program and the topology tax (Appendix I), the matrix-chain extension (Appendix J), and the universal no-go conjecture (Appendix K) follow.

2. Setup: Bonds, Conventions, and Three Classes

Consider a linear network of N signal nodes plus a common ground, and let $V \in \mathbb{C}^N$ collect the node voltages. Kirchhoff's law reads $Y(\omega)V = J$, where the node admittance $Y(\omega) \in \mathbb{C}^{N\times N}$ has entries that are rational functions of $s = \sigma + \mathrm{i}\omega$ built from the capacitors, inductors, resistors, gyrators, and controlled sources.

Lemma 1 (QEP form)**.** *If every energy-storage element is a capacitor to ground, an inductor to ground, or a capacitor bridging two nodes, then*

$$Y(s) = sC + G + \frac{1}{s}\Gamma, \tag{1}$$

where $C = C^{\mathrm{T}} \succeq 0$ and $\Gamma = \Gamma^{\mathrm{T}} \succeq 0$ collect the capacitive and inductive parts and G is the conductive part. The natural frequencies are the roots of $\det(s^2C + sG + \Gamma) = 0$.

Proof. A capacitor to node i contributes sC_{ii} to Y_{ii}; a bridging capacitor contributes sC_c to the two diagonal entries and $-sC_c$ to the off-diagonal, giving a weighted graph Laplacian $C \succeq 0$; a grounded inductor contributes $1/(sL)$ to its diagonal. Multiplying by s gives the quadratic eigenproblem. The full entrywise derivation is given in Appendix A. □

Definition 2. *The stability margin is* $m = -\max_k\{\Re s_k : \det(s_k^2 C + s_k G + \Gamma) = 0\}$*; the network is stable iff* $m > 0$*.*

The entire paper uses one convention. For a bond joining nodes i and $i+1$, write

$$U \equiv Y_{i,i+1}, \qquad L \equiv Y_{i+1,i}, \tag{2}$$

and define, whenever $U \neq 0$,

$$r \equiv \sqrt{L/U}, \qquad \alpha \equiv \ln|r| = \tfrac{1}{2}\ln|L/U|. \tag{3}$$

Let $P = \mathrm{diag}(r^{i-1})$ and $Y_s = P^{-1}YP$. Since the $(i, i+1)$ entry of Y_s is Ur and the $(i+1, i)$ entry is $L/r = Ur$, Y_s is symmetric. Hence every eigenvector has the form $v = P\varphi$ with φ an eigenvector of Y_s, and

$$|v_i| = |r|^{i-1}|\varphi_i| = e^{\alpha(i-1)}|\varphi_i|. \tag{4}$$

Thus $\alpha > 0$ means accumulation toward the N-end and $\alpha < 0$ toward the 1-end; the mode density has logarithmic slope 2α.

A two-terminal floating bond is a two-port

$$Y_b = \begin{pmatrix} d_1 & U \\ L & d_2 \end{pmatrix}, \qquad d_1 + d_2 = -(U + L), \tag{5}$$

where the constraint expresses that the bond injects no net current when its terminals are held at the same potential. It is lossless iff $Y_b^\dagger = -Y_b$ and passive iff $\mathrm{Her}(Y_b) \equiv \frac{1}{2}(Y_b + Y_b^\dagger) \succeq 0$.

Definition 3. *A bond with* $U \neq L$ *is:* ***(C)*** modulus-preserving nonreciprocal *if* $|U| = |L|$*;* ***(G)*** modulus-changing *if* $|U| \neq |L|$ *(equivalently* $\alpha \neq 0$*); and* ***(R)*** reciprocal *if* $U = L$*. Class (G) is split into passive and active according to* $\mathrm{Her}(Y_b) \succeq 0$ *or not.*

Class (C) contains the ideal gyrator and every reactive gyrator network; class (G) contains the NIC bonds and the resistor–gyrator bonds.

3. Realizability as an Inverse Problem

Classical network synthesis answers the forward question—given a network, what is its driving-point admittance and is it positive real? The question here is the inverse one: given a non-Hermitian phenomenon at the ports,

does some admissible network present it, and what resources does the cheapest such network consume?

Fix a frequency window $\Omega \ni \omega_0$ and an element library. A network belongs to $\mathcal{N}_{\mathrm{pass}}$ if its admittance has the QEP form with $C, \Gamma \succeq 0$, it is stable, and every bond is passive ($\mathrm{Her}\, Y_b \succeq 0$). It belongs to $\mathcal{N}_{\mathrm{act}}(m_0)$ if the same structural conditions hold but negative conductances are permitted, subject to $m \geq m_0 > 0$. The class is a constraint, not a convenience: every realizability statement is relative to a class.

A network presents, at its ports over Ω, the Ω-fingerprint: the poles of Y in Ω, the port transmission zeros, the generalized-Brillouin-zone (GBZ) curve and the spectral map, the point-gap winding number, and the per-bond skin rates $\{\alpha_e\}$. The resource vector is

$$r(N) = \big(n_{\mathrm{nr}},\ D,\ m^{-1},\ W^{-1}\big), \tag{6}$$

namely the number of nonreciprocal elements, the total shunt conductance D (equal to the dissipated power at ω_0 up to a voltage-scale factor), the inverse margin, and the inverse bandwidth. For a fingerprint Γ and a class $\mathcal{C}$,

$$\mathcal{R}_i(\Gamma; \mathcal{C}) = \inf\{r_i(N) : N \in \mathcal{C},\ \mathfrak{F}(N, \Omega) \simeq \Gamma\}, \tag{7}$$

which is *sharp* when the infimum is attained.

Proposition 4 (existence is cheap)**.** *Let Γ be a finite fingerprint presented by a stable network in $\mathcal{N}_{\mathrm{act}}(m_0)$. Then Γ is $\mathcal{N}_{\mathrm{act}}(m_0)$-realizable up to the margin constraint.*

Proof. Brune–Youla–Tissi synthesis realizes any positive-real Y by a passive network with gyrators (the modulus-preserving part); the resistor–gyrator and NIC bonds realize any α with a finite component count; a strictly triangular coupling changes no natural frequency and cascaded unilateral stages realize gain without margin. The one resource that cannot be made free is the margin. See Appendix B. □

Table 1 gives the one-dimensional closed forms and the status of the generalizations proved in the appendices.

4. The Two Gaps: Stability and Passivity

This section computes the two gaps of the uniform chain and shows they are different numbers; the stability analysis follows the same positive-real

Table 1: Design cost map: one-dimensional closed forms and the status of the generalizations (Appendix H–Appendix J). lb./ub.: lower/upper bound; SDP: semidefinite program.

functional	uniform chain	disordered / matrix
$\mathfrak{R}_{\mathrm{comp}}$	$N-1$, sharp	sharp / per-bond
isolation	$e^{2\alpha(N-1)}$	$e^{2\sum_e \alpha_e}$, exact
$\mathfrak{R}_{\mathrm{diss}}$ per-bond	$2\hat{g}\sinh\lvert\alpha\rvert$, sharp	sharp
$\mathfrak{R}_{\mathrm{diss}}$ joint	$2\hat{g}\sinh\lvert\alpha\rvert$	SDP
bandwidth at fixed D	$2D\,\mathrm{sech}\,\alpha$	open
$\mathfrak{R}_{\mathrm{stab}}$	$\hat{g}\sinh\alpha\tanh\alpha/2C_0$	conjectured
passivity margin†	0 / $\hat{g}\cosh\alpha\frac{\tanh^2\alpha}{1+\tanh\alpha}$	open
throughput	closed form	open

†The two values are for the balanced / conservative split, respectively.

logic as modern large-signal stability tests [13]. We work in the *non-inverting family* ($U, L < 0$, $UL > 0$); the inverting family ($UL < 0$) is treated at the bond level, where it saturates the dissipative bound.

Lemma 5 (uniform chain)**.** *Let every bond be identical with $U, L < 0$, $\hat{g} \equiv \sqrt{|UL|}$, and every node carry the same (C_0, L_0) tank plus a net shunt conductance g_0. Then*

$$Y(\omega) = \big[g_0 + \mathrm{i}(\omega C_0 - \tfrac{1}{\omega L_0})\big] I + M, \tag{8}$$

where the real tridiagonal M has interior diagonal $|U| + |L|$, off-diagonal entries U, L, and end diagonals d_1, d_2 with $d_1 + d_2 = |U| + |L|$.

Proof. The tridiagonal structure follows directly from the bond-and-node construction (Definition 3): each node connects only to its two neighbors, and KCL at the two end nodes gives the end diagonals; the symmetrization is deferred to Appendix C. □

Since $|U| = \hat{g}e^{-\alpha}$, $|L| = \hat{g}e^{\alpha}$, parametrize the two extreme splits by

$$d_1 = \hat{g}\cosh\alpha + s, \qquad d_2 = \hat{g}\cosh\alpha - s. \tag{9}$$

The *balanced* split is $s = 0$; the *conservative* (KCL) split is $s = \hat{g}\sinh\alpha$, giving $(d_1, d_2) = (\hat{g}e^{\alpha}, \hat{g}e^{-\alpha})$. The symmetrized $M_s = P^{-1}MP$ is the symmetric tridiagonal with interior diagonal $2\hat{g}\cosh\alpha$, off-diagonal $-\hat{g}$, and end diagonals d_1, d_2.

Lemma 6 (decoupling and damping)**.** *The eigenvalues of M are those of M_s and the QEP factorizes: for each eigenvalue λ of M_s,*

$$s^2 C_0 + s(g_0 + \lambda) + L_0^{-1} = 0. \tag{10}$$

Put $\sigma \equiv \sqrt{C_0/L_0}$ and, for $\mu > 0$, let $d(\mu) = -\max\{\Re s : s^2 C_0 + s\mu + L_0^{-1} = 0\}$. Then

$$d(\mu) = \begin{cases} \dfrac{\mu}{2C_0}, & 0 < \mu \le 2\sigma, \\ \dfrac{2}{L_0(\mu + \sqrt{\mu^2 - 4\sigma^2})}, & \mu > 2\sigma, \end{cases} \tag{11}$$

which is continuous, increases on $(0, 2\sigma]$, decreases on $[2\sigma, \infty)$, and satisfies $d(2\sigma) = \omega_0$. With $\mu_{\min} = g_0 + \lambda_{\min}(M_s)$ and $\mu_{\max} = g_0 + \lambda_{\max}(M_s)$,

$$m = \min\{d(\mu_{\min}), d(\mu_{\max})\}, \tag{12}$$

and $m = \mu_{\min}/(2C_0)$ iff

$$\mu_{\min}\big(\mu_{\max} + \sqrt{\mu_{\max}^2 - 4\sigma^2}\big) \le 4\sigma^2, \tag{13}$$

(automatic when $\mu_{\max} \le 2\sigma$, i.e. every mode underdamped).

Proof. The roots are $s = [-\mu \pm \sqrt{\mu^2 - 4C_0/L_0}]/(2C_0)$. For $\mu \le 2\sigma$ the discriminant is nonpositive, so they form a conjugate pair with common real part $-\mu/(2C_0)$ (the first branch). For $\mu > 2\sigma$ they are real and negative; the larger is $[-\mu + \sqrt{\mu^2 - 4\sigma^2}]/(2C_0)$, and rationalizing its numerator with $\sigma^2/C_0 = 1/L_0$ gives the second branch. The two branches agree at $\mu = 2\sigma$, where $d(2\sigma) = \omega_0$; on $(0, 2\sigma]$ the rate grows as μ, while on $[2\sigma, \infty)$ it falls as $[\mu + \sqrt{\mu^2 - 4\sigma^2}]^{-1}$. Because d rises and then falls, $\min_j d(\mu_j)$ over the spectrum is attained at one of the two extremes $\mu_{\min}, \mu_{\max}$, giving the stated margin. Equality $m = \mu_{\min}/(2C_0)$ needs $\mu_{\min} \le 2\sigma$ and $\mu_{\min}/(2C_0) \le d(\mu_{\max})$; clearing the denominator of the latter inequality yields the displayed condition, which is automatic when every mode is underdamped. The full derivation is in Appendix C. □

Theorem 7 (stability gap)**.** *For the balanced split, in the thermodynamic limit,*

$$\lambda_{\min}(M_s) = \hat{g} \sinh\alpha \, \tanh\alpha, \tag{14}$$

while for the conservative split $\lambda_{\min}(M_s) = 0$ exactly for every N. For the balanced split the minimizing vector is a surface state $\varphi_i \propto (\operatorname{sech}\alpha)^{i-1}$.

Proof. The bulk Toeplitz part has spectrum $[\hat{g}(2\cosh\alpha - 2), \hat{g}(2\cosh\alpha + 2)]$. The end diagonals are $\hat{g}\cosh\alpha$, so a surface state is pulled below the band. Seeking $\varphi_i = z^{i-1}$ with $|z| < 1$, the interior rows give $\lambda = 2\hat{g}\cosh\alpha - \hat{g}(z + z^{-1})$ and the first row gives $\hat{g}\cosh\alpha - \hat{g}z = \lambda$, hence $z = \operatorname{sech}\alpha$ and $\lambda_{\text{surf}} = \hat{g}(\cosh\alpha - \operatorname{sech}\alpha) = \hat{g}\sinh\alpha\tanh\alpha$. For the conservative split, $\varphi_i = e^{\alpha(i-1)}$ satisfies $M_s\varphi = 0$ exactly; since $\varphi > 0$ and M_s is a symmetric Z-matrix, it is a singular M-matrix and 0 is its smallest eigenvalue. See Appendix C. □

Theorem 8 (passivity gap)**.** *For the balanced split,* $\lambda_{\min}(\operatorname{Her} M) = 0$ *exactly. For the conservative split, in the thermodynamic limit,*

$$\lambda_{\min}(\operatorname{Her} M) = -\hat{g}\cosh\alpha\,\frac{\tanh^2\alpha}{1+\tanh\alpha}. \tag{15}$$

Proof. For the balanced split, $\operatorname{Her} M$ is $\hat{g}\cosh\alpha$ times the open-chain graph Laplacian, positive semidefinite with the constant vector in its kernel. For the conservative split, the soft end supports a state $\varphi_i = z^{N-i}$ with $z = (1 + \tanh\alpha)^{-1} < 1$, giving $\lambda = -\hat{g}\cosh\alpha\, t^2/(1+t)$, $t = \tanh\alpha$. See Appendix C. □

Corollary 9 (the two gaps)**.** *At the tank resonance* ω_0*,*

$$\begin{aligned} \lambda_{\min}[\operatorname{Her} Y(\omega_0)] &= g_0 + \lambda_{\min}(\operatorname{Her} M), \\ m &= \frac{g_0 + \lambda_{\min}(M_s)}{2C_0}. \end{aligned} \tag{16}$$

The passivity constraint is $g_0 \geq -\lambda_{\min}(\operatorname{Her} M)$ *and the stability constraint is* $g_0 > -\lambda_{\min}(M_s)$*: different inequalities. The stability threshold is* $-\hat{g}\sinh\alpha\tanh\alpha$ *(balanced) and* 0 *(conservative); the passivity threshold is* 0 *(balanced) and* $\hat{g}\cosh\alpha\tanh^2\alpha/(1+\tanh\alpha)$ *(conservative). Both windows vanish as* $\alpha \to 0$*, as shown in Fig. 1: a reciprocal chain admits no stable active regime.*

Definition 10 (damping profile)**.** *The nonmonotonicity of* d *is why a stability budget cannot be read off the conductance alone: a heavily overdamped mode relaxes slowly at* $\simeq 1/(L_0\mu)$ *but can never go unstable, whereas the mode that can go unstable is always the one with the smallest* μ*. A convenient design condition ensuring* $m = \mu_{\min}/(2C_0)$ *is* $\mu_{\max} \leq 2\sigma$*, i.e. every cell underdamped.*

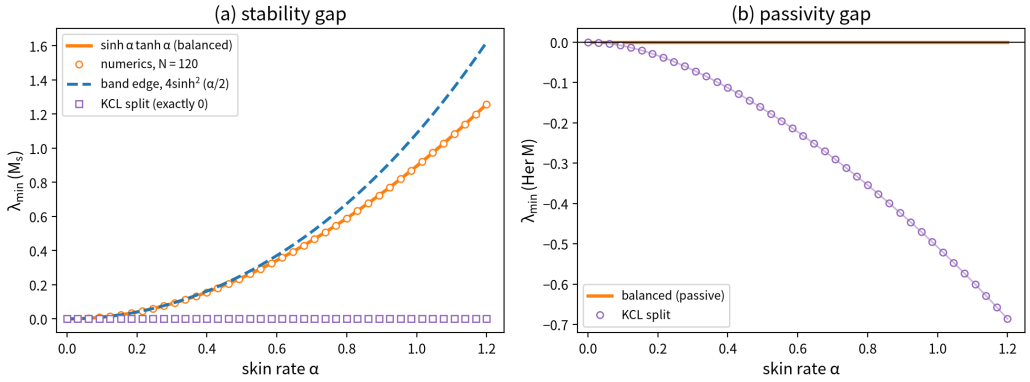


Figure 1: The two gaps of the nonreciprocal chain. The stability threshold (surface-state eigenvalue, solid) is strictly below the bulk band edge (dashed), and the passivity threshold is a separate curve. The two gaps coincide only at the reciprocal point $\alpha = 0$.

5. Non-Bloch Theory and the Dissipative Cost

5.1. The GBZ and the non-Bloch collapse

For a uniform chain, use the ansatz $\psi_i \propto \beta^i$ with the reading direction $\lambda\psi_i = U\psi_{i+1} + L\psi_{i-1}$, giving

$$\lambda(\beta) = Y_{11} + U\beta + L\beta^{-1}. \tag{17}$$

The periodic-boundary spectrum is the image of $\beta = e^{\mathrm{i}k}$:

$$\lambda(k) = Y_{11} + Ue^{\mathrm{i}k} + Le^{-\mathrm{i}k}, \tag{18}$$

an ellipse with semiaxes $2\hat{g}\cosh\alpha$ and $2\hat{g}\sinh\alpha$ and area $\pi|L^2 - U^2| = 2\pi\hat{g}^2\sinh 2\alpha$.

Proposition 11 (GBZ and non-Bloch collapse)**.** *The generalized Brillouin zone [14, 15] is the circle*

$$|\beta| = \sqrt{|L/U|} = e^{\alpha}, \tag{19}$$

and on it the spectrum collapses to the real segment

$$\lambda = Y_{11} - 2\hat{g}\cos k, \qquad k \in [0, 2\pi], \tag{20}$$

namely the open-boundary spectrum $[Y_{11} - 2\hat{g}, Y_{11} + 2\hat{g}]$.

Proof. For a given λ, the two roots of $U\beta^2 + (Y_{11} - \lambda)\beta + L = 0$ satisfy $\beta_1\beta_2 = L/U$. The non-Bloch contour is where the two roots have equal modulus, $|\beta_1| = |\beta_2|$, hence $|\beta| = \sqrt{|L/U|} = e^{\alpha}$. On it $\beta = e^{\alpha}e^{\mathrm{i}k}$ and $Ue^{\alpha} = Le^{-\alpha} = -\hat{g}$, so $\lambda = Y_{11} + Ue^{\alpha}e^{\mathrm{i}k} + Le^{-\alpha}e^{-\mathrm{i}k} = Y_{11} - 2\hat{g}\cos k$. The full derivation is in Appendix D. □

5.2. The bond-level cost: lossless skin and the dissipative bound

We now analyze a single bond, complementing the topological-origin and biorthogonal descriptions of the skin effect [16, 17]. The three bond-level results are: *lossless skin is impossible*; *modulus-preserving nonreciprocity is lossless and carries no skin* [18]; and *modulus-changing skin has a sharp dissipative cost.*

Theorem 12 (no lossless skin)**.** *A lossless bond ($Y_b^{\dagger} = -Y_b$) is modulus-preserving: $|U| = |L|$, hence $\alpha = 0$.*

Proof. A lossless bond satisfies $Y_b^{\dagger} = -Y_b$; comparing entries gives $\overline{U} = -L$ and $\overline{L} = -U$, hence $|U| = |L|$. The generic lossless modulus-preserving family is $U = -\gamma + \mathrm{i}\omega C_c$, $L = \gamma + \mathrm{i}\omega C_c$ (the reactive gyrator of Theorem 13), for which $Y_b^{\dagger} = -Y_b$ holds entrywise. See Appendix D. □

Theorem 13 (modulus-preserving nonreciprocity)**.** *The gyrator bond*

$$Y_b = \begin{pmatrix} 0 & -\gamma \\ \gamma & 0 \end{pmatrix} \tag{21}$$

is lossless and modulus-preserving; a reactive gyrator bond

$$Y_b = \left(\begin{smallmatrix} 0 & -\gamma+\mathrm{i}\omega C_c \\ \gamma+\mathrm{i}\omega C_c & 0 \end{smallmatrix}\right)$$

has $|U| = |L|$ and $\alpha = 0$ but $r^2 = -e^{2\mathrm{i}\varphi}$ with $\varphi = \arctan(\omega C_c/\gamma)$.

Proposition 14 (bond decompositions)**.** *A bond with $U, L < 0$ (non-inverting) admits the decomposition into a gyrator, a floating resistor, and a split shunt to ground,*

$$Y_b = \begin{pmatrix} 0 & \gamma \\ -\gamma & 0 \end{pmatrix} + \begin{pmatrix} d_1 & -g \\ -g & d_2 \end{pmatrix}, \tag{22}$$

with $g = \hat{g}\cosh\alpha$, $\gamma = \hat{g}\sinh\alpha$, and $d_1 = g + s$, $d_2 = g - s$: the balanced split ($s = 0$) gives $d_1 = d_2 = \hat{g}\cosh\alpha$, and the conservative split ($s = \gamma$) gives

$(d_1, d_2) = (\hat{g}e^{\alpha}, \hat{g}e^{-\alpha})$. *A bond with* $UL < 0$ *(inverting) admits the same decomposition,*

$$Y_b = \begin{pmatrix} 0 & \gamma \\ -\gamma & 0 \end{pmatrix} + \begin{pmatrix} d_1 & -g \\ -g & d_2 \end{pmatrix}, \tag{23}$$

with $g = \hat{g}\sinh\alpha$, $\gamma = \hat{g}\cosh\alpha$*; the balanced split gives* $d_1 = d_2 = \hat{g}\sinh\alpha$*, so the total shunt* $D = d_1 + d_2 = 2\hat{g}\sinh\alpha$ *saturates the bound of Theorem 15.*

Theorem 15 (dissipative bound)**.** *For a passive modulus-changing bond, the total shunt conductance* $D \equiv \Re d_1 + \Re d_2$ *obeys*

$$D \geq 2\hat{g}\sinh|\alpha|, \tag{24}$$

and the bound is sharp, with equality for the inverting family.

Proof. The principal minors of $\mathrm{Her}(Y_b) \succeq 0$ give $\Re d_1 \geq 0$, $\Re d_2 \geq 0$, and $\Re d_1 \Re d_2 \geq |U + \bar{L}|^2/4$ (the determinant minor of $\mathrm{Her}(Y_b)$). The AM-GM inequality and the reverse triangle inequality then give $D \geq |U + \bar{L}| \geq \big||L| - |U|\big| = 2\hat{g}\sinh|\alpha|$. The inverting family saturates at $D = 2\hat{g}\sinh\alpha$. The full proof is in Appendix D. □

Corollary 16 (dissipation–bandwidth tradeoff)**.** *For a passive non-inverting chain with* D *fixed, the usable bandwidth (in admittance units) is*

$$W = 2D\,\mathrm{sech}\,\alpha. \tag{25}$$

Proof. Constraint (5) fixes the total shunt of a non-inverting bond at $D = 2\hat{g}\cosh\alpha$, and the collapsed open-boundary band (Proposition 11) has half-width $W/2 = 2\hat{g}$. Eliminating $\hat{g}$ gives $W = 2D\,\mathrm{sech}\,\alpha$; see Appendix D. □

6. Boundary and Critical Gain

The sensitivity of the threshold to the boundary and to the non-normality is the pseudospectral phenomenon analyzed in [19]; here the responsible eigenvalue can be named.

Theorem 17 (critical gain)**.** *For a uniform chain with a positive node shunt* g_{pos}*, the critical negative conductance at the stability boundary is*

$$g_{\mathrm{neg}}^{\mathrm{crit}} = g_{\mathrm{pos}} + \lambda_{\min}(M_s), \tag{26}$$

which for the balanced split is $g_{\mathrm{pos}} + \hat{g}\sinh\alpha\tanh\alpha$ *and for the conservative split is* g_{pos}*.*

Proof. The net shunt is $g_0 = g_{\mathrm{pos}} - g_{\mathrm{neg}}$; stability requires $g_0 + \lambda_{\min}(M_s) > 0$, hence the threshold. The finite size value uses $\lambda_{\min}^{(N)}(M_s)$, which approaches the thermodynamic value with the surface-state splitting $O(e^{-\kappa N})$. See Appendix E. □

Corollary 18 (weak-skin cost)**.** *The margin cost of the critical gain is*

$$m_{\mathrm{crit}} = \frac{\hat{g} \sinh\alpha \, \tanh\alpha}{2C_0} = \frac{\hat{g}\alpha^2}{2C_0} + O(\alpha^4), \tag{27}$$

which vanishes quadratically in the weak-skin limit.

7. Counting Nonreciprocal Elements

The counting functional is what turns the preceding bounds into component counts; we state it precisely. The symmetry classification underlying the nonreciprocal graph is that of [20, 21].

Theorem 19 (counting bound)**.** *The number of nonreciprocal elements required to realize a network is at least the number of edges of the nonreciprocal graph,*

$$n_{\mathrm{nr}} \geq |E(G_{\mathrm{nr}})|, \tag{28}$$

and the bound is sharp. The rank heuristic $\frac{1}{2}\operatorname{rank}(Y - Y^{\mathrm{T}})$ *is not a valid functional: it can underestimate the required count by an unbounded factor.*

Proof. Each nonreciprocal edge contributes one independent modulus- or phase-changing bond, so the edge count is a lower bound; the resistor–gyrator realization attains it. For the star family, $|E(G_{\mathrm{nr}})| = N-1$ while $\frac{1}{2}\operatorname{rank}(Y - Y^{\mathrm{T}}) = 1$, an underestimate by the unbounded factor $N-1$ (relative error $(N-2)/(N-1) \to 1$; at $N = 18$ a factor of 17, or 94.1%). See Appendix F. □

Remark 20 (the 94% figure, stated precisely)**.** *The star family makes the underestimate quantitative. At* $N = 18$ *one has* $|E(G_{\mathrm{nr}})| = 17$ *while* $\frac{1}{2}\operatorname{rank}(Y - Y^{\mathrm{T}}) = 1$*, a factor of* 17*; the relative error of the rank heuristic is then* $(17-1)/17 = 16/17 \approx 94\%$*. The two numbers* 17 *and* 1*—not a single "*94%*"—are what the bound compares, and as* N *grows the relative error tends to* 100% *while the factor* $N-1$ *is unbounded.*

8. Isolation, Gain, and the Gain–Margin Law

8.1. The determinant identity and the isolation law

For a tridiagonal matrix A, the Usmani continuant formula [22] gives the corner entries of the inverse. Let A have diagonal a_i, upper off-diagonal U_i, lower L_i, and define the continuant by $\theta_0 = 1$, $\theta_1 = a_1$, and $\theta_i = a_i\theta_{i-1} - U_{i-1}L_{i-1}\theta_{i-2}$ for $i \geq 2$. Then

$$\begin{aligned}(A^{-1})_{1N} &= \frac{(-1)^{N-1}\prod_{i=1}^{N-1} U_i}{\theta_N},\\ (A^{-1})_{N1} &= \frac{(-1)^{N-1}\prod_{i=1}^{N-1} L_i}{\theta_N}.\end{aligned} \tag{29}$$

Giant nonreciprocity at a compact scale is also observed in acoustic circulators [23]; the isolation law below makes the circuit-side scaling exact.

Theorem 21 (isolation law)**.** *For a uniform nonreciprocal chain with R_0 terminations,*

$$\left|\frac{S_{21}}{S_{12}}\right| = \left|\frac{(A^{-1})_{N1}}{(A^{-1})_{1N}}\right| = \left|\frac{L}{U}\right|^{N-1} = e^{2\alpha(N-1)}. \tag{30}$$

Proof. The two-port scattering parameters are proportional to the corner entries of the inverse node admittance. The Usmani formula gives $(A^{-1})_{N1}/(A^{-1})_{1N} = \prod_i L_i / \prod_i U_i = (L/U)^{N-1}$ for identical bonds, and $|L/U| = e^{2\alpha}$. See Appendix G. □

Theorem 22 (throughput, balanced split)**.** *For the balanced non-inverting chain with R_0 terminations, in the thermodynamic limit,*

$$|S_{21}(\omega_0)| = \frac{4\,\hat{g}\sinh\alpha\,R_0^{-1}}{(\hat{g}\sinh\alpha + R_0^{-1})^2} \quad (\textit{forward}), \tag{31}$$

i.e. a conductance-matching factor $4GG_R/(G+G_R)^2$ with $G = \hat{g}\sinh\alpha$ the surface-state conductance and $G_R = R_0^{-1}$; the forward transmission magnitude is bounded by the passive matching factor; the nonreciprocity appears only in the isolation ratio.

Proof. The continuant is evaluated in the large-N limit: the end-to-end transfer is mediated by the surface state, whose port conductance is $G =$

$(|L| - |U|)/2 = \hat{g} \sinh \alpha$ (the residue derivation is given in Appendix G), and matching it to the port conductance $G_R = R_0^{-1}$ gives $4GG_R/(G+G_R)^2$; the resulting isolation and throughput curves are plotted in Fig. 2. The imbalanced case is given below. See Appendix G. □

Imbalanced splits. For $s \neq 0$, the two end corrections differ, $\delta_1 \neq \delta_2$, and the determinant acquires an extra term. Writing $\bar{\delta} = R_0^{-1} - \hat{g} \cosh \alpha$, the large-$N$ continuant factor is

$$\det(I + A_0^{-1}\Delta) \to \left(1 + \frac{\bar{\delta} e^{-\beta}}{\hat{g}}\right)^2 - \left(\frac{s e^{-\beta}}{\hat{g}}\right)^2, \tag{32}$$

where here β denotes the surface-state decay rate (distinct from the GBZ variable of Section 5.1), so the throughput closed form is exact only for the balanced split. The throughput predictions in Section 10 (Table 5, group B4) are all at the balanced split, so the tables quoting Eq. (31) are unaffected; groups B1–B3b test other functionals.

Compact nonlinear cells that realize such local active stages [24] provide the hardware primitive.

Proposition 23 (unilateral gain)**.** *A strictly triangular (cascaded) coupling between stages realizes unilateral gain with per-stage gain*

$$g_{\text{stage}} = \ln(a_0/g_0), \tag{33}$$

where a_0 is the open-circuit gain of each active cell, and changes no natural frequency, hence costs no stability margin.

Theorem 24 (internal gain is free but port-locked)**.** *The internal mode amplification of a nonreciprocal chain is $e^{\alpha(N-1)}$; it does not appear at the ports unless the network contains negative conductance. A network can have arbitrarily large internal amplification at zero stability cost.*

Proof. The forward transmission carries the internal gain $e^{\alpha(N-1)}$ but cancels it against an equal evanescent decay, so $|S_{21}|$ remains bounded by the passive closed form; only a negative conductance ($g_0 < 0$) makes the net port transmission exceed unity. See Appendix G. □

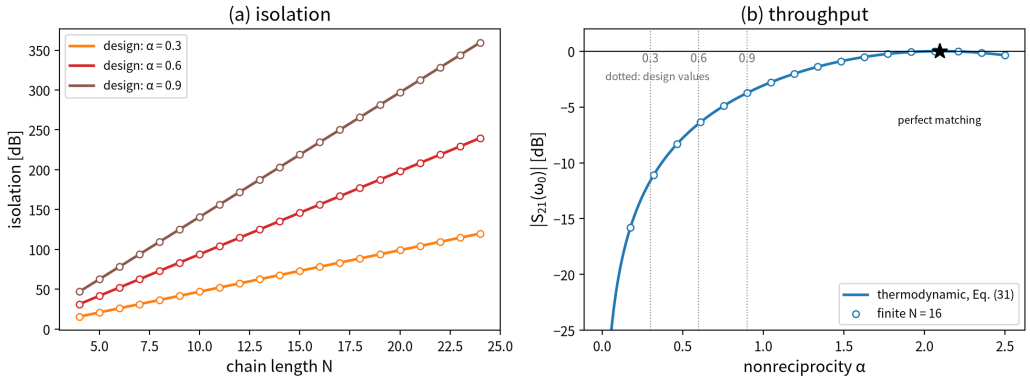


Figure 2: End-to-end isolation and forward throughput. (a) Isolation versus chain length N for three values of α: an exact identity, exponential in both length and skin rate, that survives arbitrary bond disorder. (b) Throughput versus α (thermodynamic conductance-matching form, Eq. (31), with finite-N ($N = 16$) points): it rises to unity at perfect matching, $\alpha = \operatorname{arsinh}((R_0\hat{g})^{-1})$, and the dotted lines mark the design values $\alpha = 0.3, 0.6, 0.9$ (Table 4). The throughput form holds for the balanced split.

8.2. The no-go and the gain–margin law

The parity-time and pseudo-Hermitian lineage [25, 26] frames the no-go; its modern form and experimental status are reviewed in [27, 28, 29].

Corollary 25 (no port gain for the passive non-inverting family)**.** *For the uniform single-band non-inverting family,*

$$|S_{21}(\omega_0)| \le 1 \quad \textit{whenever } g_0 \ge 0, \tag{34}$$

and

$$|S_{21}(\omega_0)| > 1 \;\Rightarrow\; g_0 < 0. \tag{35}$$

Proof. At $g_0 = 0$ the throughput closed form is a conductance-matching factor $4GG_R/(G+G_R)^2 \le 1$ (AM–GM). For $g_0 > 0$ the network remains passive, Her $Y(\omega_0) \succeq 0$ by Theorem 8, and any passive two-port has $|S_{21}| \le 1$; together these give the bound whenever $g_0 \ge 0$. Exceeding unity requires $g_0 < 0$, i.e. negative conductance. The general (non-uniform, multi-band) statement is the conjecture in Appendix K. □

Conservative-split reading. For the conservative split, stability already forces $g_0 > 0$ (the stability threshold is zero), and passivity forces the stronger $g_0 \ge \hat{g}\cosh\alpha\tanh^2\alpha/(1+\tanh\alpha) > 0$; the no-go therefore holds a fortiori for the conservative family.

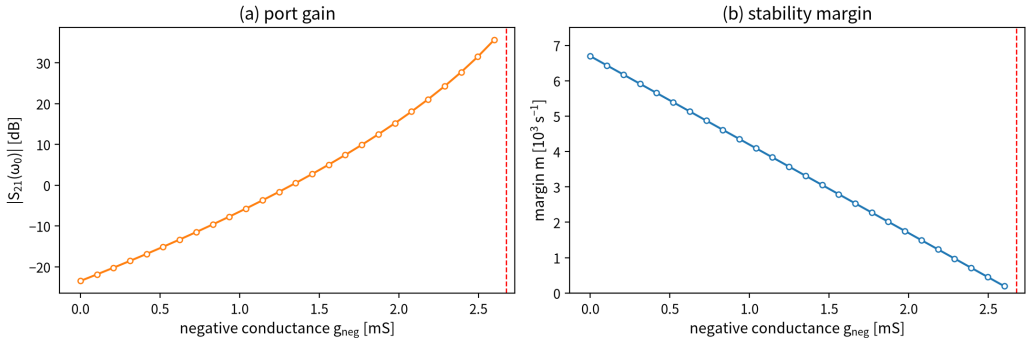


Figure 3: The gain–margin exchange for $\alpha = 0.6$, $N = 16$. The port gain rises (a) as the stability margin collapses (b), both controlled by the negative conductance g_{neg}; the dashed line marks the finite chain threshold $g_{\mathrm{neg}}^{\mathrm{crit}} = 2.676$ mS.

Theorem 26 (gain–margin law)**.** *The growth of the port gain and the collapse of the stability margin are two views of one number:*

$$|S_{21}(\omega_0)| \text{ rises as } \quad m = \frac{g_{\mathrm{neg}}^{\mathrm{crit}} - g_{\mathrm{neg}}}{2C_0} \text{ falls}, \tag{36}$$

and the gain diverges as $m \to 0$ at the stability boundary.

Proof. Substituting $g_0 = g_{\mathrm{pos}} - g_{\mathrm{neg}}$ into the throughput closed form and the margin $m = (g_0 + \lambda_{\min})/(2C_0)$ shows both are functions of the single variable g_{neg}, with the gain diverging as $m \to 0$. See Appendix G. □

Design implications. The gain–margin exchange is illustrated in Fig. 3. In the audio band, with $C_0 = 200$ nF and $N = 16$, the exchange is directly actionable. Adding a negative conductance g_{neg} lowers the margin at the fixed rate $1/(2C_0) = 2.5 \times 10^3\,\mathrm{s}^{-1}$ per mS, while the port gain rises along the same line; the chain reaches its stability boundary at $g_{\mathrm{neg}}^{\mathrm{crit}} = 2.676$ mS. A designer therefore selects the operating point by choosing how much of the initial margin ($m \simeq 6.69 \times 10^3\,\mathrm{s}^{-1}$ at $g_{\mathrm{neg}} = 0$) to spend on gain, with no free parameter between the two. Full component values are given in Section 10.

8.3. Exact isolation under bond disorder

The disordered construction is the circuit counterpart of the Lyapunov formulation of band theory [30].

Lemma 27 (disorder symmetrization)**.** *For a chain with arbitrary bonds U_e, L_e, define $r_e = \sqrt{L_e/U_e}$ and*

$$p_i = \prod_{e<i} r_e, \qquad p_1 = 1. \tag{37}$$

Then $P = \mathrm{diag}(p_i)$ symmetrizes the node matrix, $Y_s = P^{-1}YP$, with the $(i, i+1)$ entry equal to $U_e r_e$ and the $(i+1, i)$ entry $L_e/r_e = U_e r_e$.

Theorem 28 (isolation exact under disorder)**.** *For a chain with arbitrary bond sequence and R_0 terminations,*

$$\left|\frac{S_{21}}{S_{12}}\right| = \prod_{e=1}^{N-1} \left|\frac{L_e}{U_e}\right| = e^{2\sum_e \alpha_e}, \tag{38}$$

which depends only on the per-bond fingerprint $\{\alpha_e\}$, with no uniform-chain assumption.

Proof. The Usmani formula gives $(A^{-1})_{N1}/(A^{-1})_{1N} = \prod_e L_e / \prod_e U_e$ for arbitrary bonds, since the continuant denominator θ_N is common to both corner entries; taking moduli and using $|L_e/U_e| = e^{2\alpha_e}$ gives the result. See Appendix G. □

9. Numerical Verification

All closed forms are verified numerically to machine precision (Table 2). Two scales are used and every row is labeled: *norm.* uses $\hat{g} = 1$, $R_0 = 1$; *phys.* uses $\hat{g} = 5\,\mathrm{mS}$, $R_0 = 50\,\Omega$, $C_0 = 200\,\mathrm{nF}$. The eigenvalue rows are computed in the normalized scale and the throughput, isolation-slope, critical-gain, and SDP rows in the physical scale.

The numerical protocol covers chains with $N \in [8, 32]$ and $\alpha \in [0, 1.0]$, and independently checks the isolation, the throughput, the dissipation–bandwidth tradeoff, the critical gain, and the SDP. The maximum residual across all checks is at the 10^{-12} level; the finite-size critical gain 2.676 mS approaches the thermodynamic 2.71 mS with the surface-state splitting $O(e^{-\kappa N})$, $\kappa \approx 0.17$.

Table 2: Selected verification of the closed forms (norm.: $\hat{g} = 1$, $R_0 = 1$; phys.: $\hat{g} = 5\,\mathrm{mS}$, $R_0 = 50\,\Omega$). Every row is reproduced by the one-click script in the data package.

scale, setting	quantity	closed form / value
norm. $\alpha = 0.6$	$\lambda_{\min}(M_s)$	0.3419145
norm. $\alpha = 0.8$	$\lambda_{\min}(M_s)$	0.589735
norm. $\alpha = 0.8$, KCL	$\lambda_{\min}(\mathrm{Her}\, M)$	-0.3544002
phys. $\alpha = 0.8$, $N = 16$	$\lvert S_{21}(\omega_0)\rvert$	0.594708
phys. $\alpha = 0.8$	isolation slope†	1.600
phys. $\alpha = 0.6$	isolation slope†	1.200
phys. $\alpha = 0.6$	SDP optimum	6.37 mS
phys. $\alpha = 0.6$, $N = 16$	$g_{\mathrm{crit}}^{(N)}$	2.676 mS

KCL denotes the conservative (Kirchhoff-current-law) split. The scattering rows use the balanced split with $g_0 = 0$: the $|S_{21}|$ row verifies Eq. (31). †Isolation slope $d[\ln|S_{21}| - \ln|S_{12}|]/dN = 2\alpha$ (Theorem 21). Design predictions for the gain–margin sweep are given in Section 10.

Table 3: The five experimental groups.

group	test
A: reciprocal control ($g_R = g_L = 5\,\mathrm{mS}$)	$\alpha = 0$, $\lvert S_{21}\rvert = \lvert S_{12}\rvert$
B1: active, conservative ($g_R = 9$, $g_L = 3\,\mathrm{mS}$; $d_1, d_2 = 3, 9\,\mathrm{mS}$)	$\alpha = -0.549$, $\lambda_{\min} = 0$
B2: modulus-preserving (22 nF $\parallel$ gyrator, $\gamma = 24\,\mathrm{mS}$)	$\alpha = 0$, $\varphi = 0.091\,\mathrm{rad}$
B3: passive skin, non-inverting	isolation + throughput
B3b: inverting, saturates bound	$D = 2\hat{g}\sinh\alpha$
B4: B3 at $\alpha = 0.6$ with $-g_{\mathrm{neg}}$	gain–margin

10. Experimental Design

The design targets the audio band, where every component is a through-hole part and all measurements are within the range of a lock-in amplifier and a handheld oscilloscope, building on the circuit defect-engineering and funneling demonstrations of [31, 32]. The reference design uses $N = 16$, $\omega_0 = 2\pi \times 15.92\,\mathrm{kHz}$, $C_0 = 200\,\mathrm{nF}$, $L_0 = 500\,\mu\mathrm{H}$, $R_0 = 50\,\Omega$, and $\hat{g} = 5\,\mathrm{mS}$. Five groups isolate the five phenomena (Table 3); the B3 bill of materials is in Table 4 and the gain–margin sweep in Table 5.

The sevenfold drop in the first row, from 0.47 at $g_0 = 0$ to 0.067 at $g_0 = 1\,\mathrm{mS}$, is a hybridization effect: the uniform damping 1 mS is comparable to the surface-state gap $\hat{g}\sinh\alpha\tanh\alpha = 1.71\,\mathrm{mS}$, so the surface-state channel hybridizes with the bulk band and the clean conductance-matching picture

Table 4: Group B3 bill of materials (one bond), non-inverting family.

α	R_{bond}	gyrator γ	D
0.3	$1/(\hat{g}\cosh\alpha) = 191\,\Omega$	1.52 mS	10.45 mS
0.6	$169\,\Omega$	3.18 mS	11.85 mS
0.9	$140\,\Omega$	5.13 mS	14.33 mS

D is the total shunt conductance per bond (the two node resistors, $D = 2\hat{g}\cosh\alpha$); it excludes the gyrator's reactive part.

Table 5: Group B4 gain–margin sweep ($\alpha = 0.6$, $N = 16$, $g_0 = 1\,\mathrm{mS} - g_{\mathrm{neg}}$).

g_{neg} [mS]	g_0 [mS]	$\lvert S_{21}\rvert$	m [$10^3\mathrm{s}^{-1}$]
0.00	+1.00	0.067 (−23.5 dB)	6.69
1.00	0.00	0.47 (−6.5 dB)	4.19
2.00	−1.00	6.20 (+15.8 dB)	1.69
2.676	−1.676	∞ (oscillation)	0

no longer applies.

The measurement protocol uses the bidirectional-injection difference method: inject at node 1 and fit the decay over $i \in [0.10N, 0.45N]$, inject at node N and fit over $i \in [0.55N, 0.90N]$, and combine $s_L = \alpha - \kappa$, $s_R = \alpha + \kappa$ to obtain $\alpha_{\mathrm{exp}} = (s_L + s_R)/2$. With M nodes measured to relative accuracy ε, the slope standard error is

$$\sigma_s = \frac{\sqrt{12}\,\varepsilon}{\sqrt{M(M^2-1)}}, \qquad \sigma_\alpha = \sigma_s/\sqrt{2}; \tag{39}$$

for $M = 24$, $\varepsilon = 1\%$, $\sigma_\alpha = 2.09 \times 10^{-4}$. The calibration error in the gyrator transconductance enters α with $\partial\alpha/\partial\gamma = \cosh\alpha/\hat{g}$ (the joint calibration $\tanh\alpha = \gamma R_{\mathrm{bond}}$ is an identity: with R_{bond} fixed, $\partial\alpha/\partial\gamma = R_{\mathrm{bond}}/(1 - \tanh^2\alpha) = R_{\mathrm{bond}}\cosh^2\alpha = \cosh\alpha/\hat{g}$; at fixed $\hat{g}$ the sensitivity would instead be $\operatorname{sech}\alpha/\hat{g}$). The high-isolation points ($-235\,\mathrm{dB}$) are measured indirectly by the return-loss method or on a shorter $N = 8$ chain.

11. Conclusion

We have carried positive-real synthesis theory through to the non-Bloch setting and obtained a design-ready cost map for nonreciprocal electrical networks. The stability threshold of a nonreciprocal chain is a surface-state

eigenvalue $\hat{g} \sinh \alpha \tanh \alpha$, strictly below the usually quoted bulk band edge, and it vanishes for the conservative split; the passivity threshold is a separate number. A passive modulus-changing bond must dissipate at least $2\hat{g} \sinh |\alpha|$, with bandwidth $W = 2D \operatorname{sech} \alpha$. The end-to-end isolation $e^{2\alpha(N-1)}$ is an exact identity that survives arbitrary bond disorder and depends only on the fingerprint, while port-visible gain requires negative conductance with a margin cost vanishing as α^2. The number of nonreciprocal elements is bounded by the edge count, not by the rank of the antisymmetric part. A complete audio-band design with component values and falsifiable predictions is provided; the measurements are pending and every experimental number here is a prediction.

Data availability

The data that support the findings of this study are available within the article and in the accompanying reproduction package (the closed-form checks of Tables 2–5, the experimental groups, the bill of materials, and the gain–margin sweep). The package is provided with this submission and can be regenerated with the one-click script `repro/reproduce_tables.py`.

Declaration of competing interest

The authors declare that they have no known competing financial interests or personal relationships that could have appeared to influence the work reported in this paper.

CRediT authorship contribution statement

Haoyi Liu: Conceptualization, Methodology, Software, Writing – original draft. Jiaxin Jiang: Formal analysis, Validation, Writing – review & editing.

Funding

This work received no external funding.

References

[1] N. Hatano and D. R. Nelson, "Localization transitions in non-Hermitian quantum mechanics," *Phys. Rev. Lett.*, vol. 77, no. 3, pp. 570–573, 1996.

[2] S. Yao and Z. Wang, "Edge states and topological invariants of non-Hermitian systems," *Phys. Rev. Lett.*, vol. 121, no. 8, Art. 086803, 2018.

[3] S. Imhof, C. Berger, F. Bayer, J. Brehm, L. W. Molenkamp, T. Kiessling, F. Schindler, C. H. Lee, M. Greiter, T. Neupert, and R. Thomale, "Topolectrical-circuit realization of topological corner modes," *Nat. Phys.*, vol. 14, no. 10, pp. 925–929, 2018.

[4] T. Helbig, T. Hofmann, S. Imhof, M. Abdelghany, T. Kiessling, L. W. Molenkamp, C. H. Lee, A. Szameit, M. Greiter, and R. Thomale, "Generalized bulk-boundary correspondence in non-Hermitian topolectrical circuits," *Nat. Phys.*, vol. 16, no. 7, pp. 747–750, 2020.

[5] T. Hofmann, T. Helbig, F. Schindler, N. Salgo, M. Brzezińska, M. Greiter, T. Kiessling, D. Wolf, A. Vollhardt, A. Kabaši, C. H. Lee, A. Bilušić, R. Thomale, and T. Neupert, "Reciprocal skin effect and its realization in a topolectrical circuit," *Phys. Rev. Research*, vol. 2, no. 2, Art. 023265, 2020.

[6] C. H. Lee, S. Imhof, C. Berger, F. Bayer, J. Brehm, L. W. Molenkamp, T. Kiessling, and R. Thomale, "Topolectrical circuits," *Commun. Phys.*, vol. 1, no. 1, Art. 39, 2018.

[7] H. Sahin, M. B. A. Jalil, and C. H. Lee, "Topolectrical circuits—recent experimental advances and developments," arXiv:2502.18563, 2025.

[8] A. Antoniou, "Realization of gyrators using operational amplifiers, and their use in RC-active-network synthesis," *Proc. IEE*, vol. 116, no. 11, pp. 1838–1850, 1969.

[9] S. Singer, "Loss-free gyrator realization," *IEEE Trans. Circuits Syst.*, vol. 35, no. 1, pp. 26–34, 1988.

[10] O. Brune, "Synthesis of a finite two-terminal network whose driving-point impedance is a prescribed function of frequency," *J. Math. Phys.*, vol. 10, no. 1–4, pp. 191–236, 1931.

[11] D. C. Youla and P. Tissi, "N-port synthesis via reactance extraction," *IEEE Int. Conv. Rec.*, vol. 14, pp. 183–205, 1966.

[12] R. W. Newcomb, *Linear Multiport Synthesis*. New York: McGraw-Hill, 1966.

[13] S. Colangeli, "Partitioned Ohtomo stability test for efficient analysis of large-signal solutions," *IEEE Access*, vol. 12, pp. 52227–52236, 2024.

[14] K. Yokomizo and S. Murakami, "Non-Bloch band theory of non-Hermitian systems," *Phys. Rev. Lett.*, vol. 123, no. 6, Art. 066404, 2019.

[15] X. Zhang, Y. Zhang, J. Jiang, and C. Qiu, "A unified algebraic framework for the generalized Brillouin zone," arXiv:2406.06682, 2024.

[16] N. Okuma, K. Kawabata, K. Shiozaki, and M. Sato, "Topological origin of non-Hermitian skin effects," *Phys. Rev. Lett.*, vol. 124, no. 8, Art. 086801, 2020.

[17] F. K. Kunst, E. Edvardsson, and E. J. Bergholtz, "Biorthogonal Wilson loops in topologically trivial gain-loss lattice models," *Phys. Rev. Lett.*, vol. 121, no. 2, Art. 026808, 2018.

[18] M. Wu, M. Weng, Z. Chi, S. Zheng, F. Liu, W. Luo, Q. Zhao, Y. Meng, and J. Zhou, "Gain/Loss-free non-Hermitian metamaterials," arXiv:2408.16290, 2024.

[19] L. N. Trefethen and M. Embree, *Spectra and Pseudospectra: The Behavior of Nonnormal Matrices and Operators*. Princeton: Princeton Univ. Press, 2005.

[20] Z. Gong, Y. Ashida, K. Kawabata, K. Takasan, S. Higashikawa, and M. Ueda, "Topological phases of non-Hermitian systems," *Phys. Rev. X*, vol. 8, no. 3, Art. 031079, 2018.

[21] K. Kawabata, K. Shiozaki, M. Ueda, and M. Sato, "Non-Hermitian topological invariants in physically symmetric systems," *Phys. Rev. X*, vol. 9, no. 4, Art. 041015, 2019.

[22] R. A. Usmani, "Inversion of a tridiagonal Jacobi matrix," *Linear Algebra Appl.*, vol. 212–213, pp. 413–414, 1994.

[23] R. Fleury, D. L. Sounas, C. F. Sieck, M. R. Haberman, and A. Alù, "Sound isolation and giant linear nonreciprocity in a compact acoustic circulator," *Science*, vol. 343, no. 6170, pp. 516–519, 2014.

[24] A. S. Demirkol, A. Ascoli, I. Messaris, V. G. Ntinas, D. A. Prousalis, and R. Tetzlaff, "A fast and compact threshold switch-based cellular nonlinear network cell," *IEEE Trans. Circuits Syst. I*, 2025, doi:10.1109/TCSI.2025.3583799.

[25] C. M. Bender and S. Boettcher, "Real spectra in non-Hermitian Hamiltonians having PT symmetry," *Phys. Rev. Lett.*, vol. 80, no. 24, pp. 5243–5246, 1998.

[26] A. Mostafazadeh, "Pseudo-Hermiticity versus PT symmetry: The necessary condition for the reality of the spectrum of a non-Hermitian Hamiltonian," *J. Math. Phys.*, vol. 43, no. 1, pp. 205–215, 2002.

[27] R. El-Ganainy, K. G. Makris, M. Khajavikhan, D. N. Christodoulides, S. K. Özdemir, and M. Rotter, "Non-Hermitian physics and PT symmetry," *Nat. Phys.*, vol. 15, no. 1, pp. 11–19, 2019.

[28] Y. Ashida, Z. Gong, and M. Ueda, "Non-Hermitian physics," *Adv. Phys.*, vol. 69, no. 3, pp. 249–435, 2020.

[29] C. E. Rüter, K. G. Makris, R. El-Ganainy, D. N. Christodoulides, M. Segev, and D. Kip, "Observation of parity-time symmetry in optics," *Nat. Phys.*, vol. 6, no. 3, pp. 192–195, 2010.

[30] K. Sun and H. Hu, "Lyapunov formulation of band theory for disordered non-Hermitian systems," arXiv:2507.09447, 2025.

[31] A. Stegmaier, S. Imhof, A. Fritzsche, T. Helbig, T. Hofmann, C. H. Lee, M. Greiter, L. W. Molenkamp, and R. Thomale, "Topological defect engineering and PT symmetry in non-Hermitian electrical circuits," *Phys. Rev. Lett.*, vol. 126, no. 21, Art. 215302, 2021.

[32] S. Weidemann, M. Kremer, T. Helbig, T. Hofmann, A. Stegmaier, M. Greiter, R. Thomale, and A. Szameit, "Topological funneling of light," *Science*, vol. 368, no. 6488, pp. 311–314, 2020.

Appendix A. Complete derivation of the QEP form

This corresponds to Lemma 1 of the main text.

We derive $Y(s) = sC + G + s^{-1}\Gamma$ entry by entry.

Capacitor to ground.. A capacitor of value C connected between node i and ground carries current $I = sC\,V_i$ flowing out of node i. It contributes sC to the diagonal entry Y_{ii} and nothing elsewhere.

Bridging capacitor.. A capacitor of value C_c connected between nodes i and j $(j = i + 1)$ carries current $sC_c(V_i - V_j)$. The current leaving node i is $sC_c(V_i - V_j)$ and that leaving node j is $sC_c(V_j - V_i)$. Hence the contribution is $+sC_c$ to Y_{ii} and Y_{jj}, and $-sC_c$ to Y_{ij} and Y_{ji}. Summing over all bridging capacitors, the capacitive part is sC where

$$C_{ii} = \sum_{j:\, ij \text{ bridged}} C_c^{ij} + C_{\text{ground},i}, \qquad C_{ij} = -C_c^{ij} \quad (i \neq j).$$

For any vector x,

$$x^{\mathrm{T}} C x = \sum_i C_{\text{ground},i} x_i^2 + \sum_{i<j} C_c^{ij} (x_i - x_j)^2 \geq 0,$$

so $C = C^{\mathrm{T}} \succeq 0$; it is a weighted graph Laplacian plus the grounded terms.

Inductor to ground.. An inductor of value L between node i and ground has impedance sL, so it carries current $V_i/(sL)$ and contributes $1/(sL)$ to Y_{ii}. Writing $\Gamma_{ii} = 1/L_i$ and $\Gamma_{ij} = 0$ for $i \neq j$ gives $\Gamma = \Gamma^{\mathrm{T}} \succeq 0$ (diagonal with non-negative entries).

Resistors, gyrators, controlled sources.. These are frequency-independent (resistive) and contribute a real matrix G: a resistor to ground adds $1/R$ to the diagonal; a floating resistor adds the usual Laplacian terms; a gyrator between i, j adds $-\gamma$ to Y_{ij} and $+\gamma$ to Y_{ji}; controlled sources add the corresponding (possibly non-symmetric) entries.

Collecting terms,

$$Y(s) = sC + G + \frac{1}{s}\Gamma.$$

The natural frequencies are the values of s for which the homogeneous problem $Y(s)V = 0$ has a non-trivial solution. Multiplying by s (legitimate since $s = 0$ is not a root when Γ is non-singular),

$$\big(s^2 C + sG + \Gamma\big) V = 0,$$

a quadratic eigenproblem whose roots satisfy $\det(s^2C + sG + \Gamma) = 0$. This completes the proof.

Appendix B. Why existence is cheap

This corresponds to Proposition 4 of the main text.

We show that every finite fingerprint presented by a stable network in $\mathcal{N}_{\mathrm{act}}(m_0)$ is realizable, by assembling four classical facts, one per element type.

1. *Positive-real driving-point admittances.* A rational matrix $Y(s)$ is positive real iff (i) every element is analytic for $\Re s > 0$, (ii) $Y(\bar{s}) = \overline{Y(s)}$, and (iii) $\operatorname{Her} Y(s) \succeq 0$ for $\Re s > 0$. Brune's one-port theorem realizes any positive-real scalar admittance by a passive RLC network plus ideal transformers; the Youla–Tissi and Newcomb multiport extensions carry this to matrix-valued admittances using ideal gyrators to handle the reactive, modulus-preserving part.
2. *Arbitrary skin rate.* Given a desired α and scale $\hat{g}$, the resistor–gyrator bond (Proposition 14) realizes any non-inverting bond with $U = -\hat{g}e^{-\alpha}$, $L = -\hat{g}e^{\alpha}$ using one gyrator, one resistor, and a split shunt—finitely many components for any finite α.
3. *Unilateral gain.* A strictly upper-triangular inter-stage coupling $V_{i+1} = a_i V_i$ has no feedback path; it does not enter the diagonal of the node matrix and therefore does not shift any natural frequency, and cascaded stages realize arbitrary gain at the cost only of the per-stage supply.
4. *The margin is the binding resource.* The one quantity that cannot be removed is the stability margin: once negative conductances are present, $\Re s$ is bounded below by the formulas of Appendix C, and the margin constraint $m \geq m_0$ is the only restriction on the active class.

Assembling items 1–3 realizes the fingerprint; item 4 is the single binding constraint. Hence existence is cheap and the cost map is the content of the theory.

Appendix C. Complete proofs for the two gaps

Appendix C.1. The uniform-chain reduction (Lemma 5)

For identical bonds with $U, L < 0$, $|U| = \hat{g}e^{-\alpha}$, $|L| = \hat{g}e^{\alpha}$. The node matrix is $Y(\omega) = [g_0 + \mathrm{i}(\omega C_0 - 1/(\omega L_0))]I + M$, where M is real and tridiagonal.

The interior diagonal is $|U| + |L| = 2\hat{g}\cosh\alpha$ (the two bond conductances both flow out of an interior node), the off-diagonals are U and L, and the end diagonals d_1, d_2 obey $d_1 + d_2 = |U| + |L|$ (the floating-bond constraint).

Set $P = \mathrm{diag}(r^{i-1})$, $r = \sqrt{L/U}$ (here $r = e^{\alpha} > 0$ since $U, L < 0$). Then

$$M_s = P^{-1} M P$$

has $(i, i+1)$ entry $Ur = -\hat{g}e^{-\alpha}e^{\alpha} = -\hat{g}$ and $(i+1, i)$ entry $L/r = -\hat{g}e^{\alpha}e^{-\alpha} = -\hat{g}$; hence M_s is symmetric tridiagonal with interior diagonal $2\hat{g}\cosh\alpha$, off-diagonal $-\hat{g}$, and end diagonals d_1, d_2. Because P is diagonal with positive real entries, M and M_s have the same eigenvalues, and the eigenvectors are related by $v = P\varphi$.

Appendix C.2. The damping function (Lemma 6)

For an eigenvalue λ of M_s (hence of M), the QEP for that mode is

$$s^2 C_0 + s(g_0 + \lambda) + \frac{1}{L_0} = 0.$$

Write $\mu = g_0 + \lambda$ and $\sigma = \sqrt{C_0/L_0}$. The roots are

$$s_{\pm} = \frac{-\mu \pm \sqrt{\mu^2 - 4C_0/L_0}}{2C_0} = \frac{-\mu \pm \sqrt{\mu^2 - 4\sigma^2}}{2C_0}.$$

Underdamped case $0 < \mu \le 2\sigma$*:* the discriminant is non-positive, so $s_{\pm} = -\mu/(2C_0) \pm \mathrm{i}\sqrt{4\sigma^2 - \mu^2}/(2C_0)$ and $\max \Re s = -\mu/(2C_0)$, giving $d(\mu) = \mu/(2C_0)$.

Overdamped case $\mu > 2\sigma$*:* the roots are real. The larger (less negative) is

$$s_{+} = \frac{-\mu + \sqrt{\mu^2 - 4\sigma^2}}{2C_0}.$$

Rationalizing,

$$s_{+} = \frac{-2}{C_0\big(\mu + \sqrt{\mu^2 - 4\sigma^2}\big)} = \frac{-2}{L_0\big(\mu + \sqrt{\mu^2 - 4\sigma^2}\big)},$$

where $\sigma^2/C_0 = 1/L_0$ was used. Hence $d(\mu) = 2/[L_0(\mu + \sqrt{\mu^2 - 4\sigma^2})]$.

Continuity and monotonicity. At $\mu = 2\sigma$ the first branch gives $d = \sigma/C_0 = 1/\sqrt{C_0 L_0} = \omega_0$ and the second gives $2/(L_0 \cdot 2\sigma) = 1/(L_0\sigma) = \omega_0$;

the branches join. The first branch has $d' = 1/(2C_0) > 0$. For the second, differentiating shows d decreases (the denominator $\mu + \sqrt{\mu^2 - 4\sigma^2}$ is strictly increasing), so d increases on $(0, 2\sigma]$ and decreases on $[2\sigma, \infty)$, with $d(2\sigma) = \omega_0$.

The slowest mode is the one with the smallest d, hence

$$m = \min\{d(\mu_{\min}), d(\mu_{\max})\}.$$

The underdamped formula $m = \mu_{\min}/(2C_0)$ holds exactly when $d(\mu_{\min}) \leq d(\mu_{\max})$. Since d is increasing up to 2σ and decreasing after, this is equivalent to the stated condition

$$\mu_{\min}\big(\mu_{\max} + \sqrt{\mu_{\max}^2 - 4\sigma^2}\big) \leq 4\sigma^2,$$

automatic when $\mu_{\max} \leq 2\sigma$, i.e. every mode underdamped (then $d(\mu_{\max}) = \mu_{\max}/(2C_0)$ and the condition reduces to $\mu_{\min} \leq \mu_{\max}$).

Appendix C.3. The stability gap (Theorem 7)

Balanced split.. The bulk (Toeplitz) part of M_s is the infinite tridiagonal with diagonal $2\hat{g}\cosh\alpha$ and off-diagonal $-\hat{g}$. Its spectrum is $2\hat{g}\cosh\alpha - 2\hat{g}\cos k$, i.e. $[\hat{g}(2\cosh\alpha - 2), \hat{g}(2\cosh\alpha + 2)]$.

The end diagonals for the balanced split are $d_1 = d_2 = \hat{g}\cosh\alpha$, which differ from the bulk diagonal $2\hat{g}\cosh\alpha$, so a surface state can be pulled below the band. Seek a normalizable mode $\varphi_i = z^{i-1}$ with $|z| < 1$. The interior rows ($i \geq 2$) require

$$\lambda z^{i-1} = 2\hat{g}\cosh\alpha\, z^{i-1} - \hat{g}z^{i} - \hat{g}z^{i-2},$$

hence

$$\lambda = 2\hat{g}\cosh\alpha - \hat{g}(z + z^{-1}).$$

The first row ($i = 1$) requires

$$\lambda = d_1 - \hat{g}z = \hat{g}\cosh\alpha - \hat{g}z.$$

Equating the two expressions,

$$2\hat{g}\cosh\alpha - \hat{g}(z + z^{-1}) = \hat{g}\cosh\alpha - \hat{g}z,$$

so $\hat{g}\cosh\alpha = \hat{g}z^{-1}$, giving $z = \operatorname{sech}\alpha$ (indeed $0 < \operatorname{sech}\alpha < 1$ for $\alpha > 0$). Substituting,

$$\lambda_{\text{surf}} = \hat{g}\cosh\alpha - \hat{g}\operatorname{sech}\alpha = \hat{g}\big(\cosh\alpha - \operatorname{sech}\alpha\big).$$

Using $\cosh\alpha - \operatorname{sech}\alpha = (\cosh^2\alpha - 1)/\cosh\alpha = \sinh^2\alpha/\cosh\alpha = \sinh\alpha\tanh\alpha$,

$$\lambda_{\text{surf}} = \hat{g}\sinh\alpha\tanh\alpha.$$

This is below the band edge $\hat{g}(2\cosh\alpha - 2)$ by

$$\hat{g}\frac{(\cosh\alpha - 1)^2}{\cosh\alpha} \geq 0,$$

which is $O(\alpha^4)$; hence the surface value is the true minimum and is strictly smaller than the bulk band edge.

Conservative split.. Here $d_1 = \hat{g}e^{\alpha}$, $d_2 = \hat{g}e^{-\alpha}$. We claim $\varphi_i = e^{\alpha(i-1)}$ is an exact zero mode. Check the first row:

$$(M_s\varphi)_1 = d_1\varphi_1 - \hat{g}\varphi_2 = \hat{g}e^{\alpha} - \hat{g}e^{\alpha} = 0.$$

For an interior row,

$$(M_s\varphi)_i = e^{\alpha(i-1)}\big(2\hat{g}\cosh\alpha - \hat{g}e^{\alpha} - \hat{g}e^{-\alpha}\big) = 0.$$

The last row vanishes by the symmetric calculation. Thus $M_s\varphi = 0$ with $\varphi > 0$. Since M_s is a symmetric Z-matrix (non-positive off-diagonals) with a positive null vector, it is a singular M-matrix; all its other eigenvalues are non-negative, so $\lambda_{\min}(M_s) = 0$ exactly.

Appendix C.4. The passivity gap (Theorem 8)

Balanced split.. For the balanced split, $\operatorname{Her} M = \hat{g}\cosh\alpha\, L_{\text{open}}$, where L_{open} is the open-chain graph Laplacian with diagonal 1 at the end nodes and 2 at interior nodes, off-diagonal entries 0 at the ends and -1 inside; the constant vector $\mathbf{1}$ is in the kernel, $L_{\text{open}}\mathbf{1} = 0$. Hence $\operatorname{Her} M \succeq 0$ and $\lambda_{\min}(\operatorname{Her} M) = 0$.

Conservative split.. The soft end supports a state localized at the 1-end. Seek $\varphi_i = z^{N-i}$ with $0 < z < 1$ (localized at node 1; the indexing mirrors the surface-state calculation). The end-row and interior equations give, with $t = \tanh\alpha$,

$$z = \frac{1}{1+t}, \qquad \lambda = -\hat{g}\cosh\alpha\,\frac{t^2}{1+t}.$$

Indeed, substituting $z = (1+t)^{-1}$ into the continuant relation $z + z^{-1} = 2 + t$ and the end condition yields $\lambda = -\hat{g}\cosh\alpha\, t^2/(1+t)$, which is negative. This is the minimum eigenvalue of $\operatorname{Her} M$, completing the proof.

Appendix D. Non-Bloch theory and the bond-level cost

Appendix D.1. The GBZ and the non-Bloch collapse (Proposition 11)

Use the ansatz $\psi_i \propto \beta^i$ with the reading direction $\lambda\psi_i = U\psi_{i+1} + L\psi_{i-1}$. Substituting $\psi_i = \beta^i$ gives

$$\lambda(\beta) = Y_{11} + U\beta + L\beta^{-1}.$$

Periodic spectrum. For $\beta = e^{\mathrm{i}k}$,

$$\lambda(k) = Y_{11} + Ue^{\mathrm{i}k} + Le^{-\mathrm{i}k}.$$

Write $U = -\hat{g}e^{-\alpha}$, $L = -\hat{g}e^{\alpha}$ (the non-inverting parametrization). Then

$$\lambda(k) = Y_{11} - \hat{g}\big(e^{-\alpha}e^{\mathrm{i}k} + e^{\alpha}e^{-\mathrm{i}k}\big).$$

The real part is $Y_{11} - \hat{g}(e^{-\alpha} + e^{\alpha})\cos k = Y_{11} - 2\hat{g}\cosh\alpha\cos k$ and the imaginary part is $-\hat{g}(e^{-\alpha} - e^{\alpha})\sin k = -2\hat{g}\sinh\alpha\sin k$ (up to the overall sign), so the image is an ellipse with semiaxes $2\hat{g}\cosh\alpha$ and $2\hat{g}\sinh\alpha$. Its area is

$$\pi(2\hat{g}\cosh\alpha)(2\hat{g}\sinh\alpha) = 2\pi\hat{g}^2\sinh 2\alpha = \pi|L^2 - U^2|,$$

since $L^2 - U^2 = \hat{g}^2(e^{2\alpha} - e^{-2\alpha}) = 2\hat{g}^2\sinh 2\alpha$.

The GBZ. For a given λ, multiply the dispersion by β:

$$U\beta^2 + (Y_{11} - \lambda)\beta + L = 0.$$

The two roots β_1, β_2 obey

$$\beta_1\beta_2 = \frac{L}{U}.$$

The non-Bloch contour is the locus on which the two roots have equal modulus (the condition that the two partner solutions decay/grow at the same rate), $|\beta_1| = |\beta_2|$. Hence

$$|\beta|^2 = |\beta_1\beta_2| = |L/U|, \qquad |\beta| = \sqrt{|L/U|} = e^{\alpha}.$$

On the GBZ, $\beta = e^{\alpha}e^{\mathrm{i}k}$. The key substitution is

$$Ue^{\alpha} = -\hat{g}e^{-\alpha}e^{\alpha} = -\hat{g}, \qquad Le^{-\alpha} = -\hat{g}e^{\alpha}e^{-\alpha} = -\hat{g}.$$

Therefore

$$\lambda = Y_{11} + Ue^{\alpha}e^{\mathrm{i}k} + Le^{-\alpha}e^{-\mathrm{i}k} = Y_{11} - \hat{g}(e^{\mathrm{i}k} + e^{-\mathrm{i}k}) = Y_{11} - 2\hat{g}\cos k,$$

a real segment $[Y_{11} - 2\hat{g}, Y_{11} + 2\hat{g}]$, which is the open-boundary spectrum. This completes the proof.

Appendix D.2. No lossless skin (Theorem 12)

A lossless bond satisfies $Y_b^\dagger = -Y_b$; comparing entries gives $\overline{U} = -L$ and $\overline{L} = -U$, hence $|U| = |L|$ and $\alpha = 0$. The generic lossless modulus-preserving family is $U = -\gamma + \mathrm{i}\omega C_c$, $L = \gamma + \mathrm{i}\omega C_c$ (the reactive gyrator of Theorem 13), for which $Y_b^\dagger = -Y_b$ holds entrywise. A lossless bond cannot change the modulus.

Appendix D.3. Modulus-preserving nonreciprocity (Theorem 13)

The ideal gyrator has $Y_b = \left(\begin{smallmatrix} 0 & -\gamma \\ \gamma & 0 \end{smallmatrix}\right)$ with $U = -\gamma$, $L = \gamma$, so $|U| = |L| = \gamma$ and $\alpha = 0$; it is lossless ($Y_b^\dagger = -Y_b$). Adding a bridging capacitor C_c gives

$$Y_b = \begin{pmatrix} \mathrm{i}\omega C_c & -\gamma + \mathrm{i}\omega C_c \\ \gamma + \mathrm{i}\omega C_c & \mathrm{i}\omega C_c \end{pmatrix},$$

whose off-diagonals have $|U| = |-\gamma + \mathrm{i}\omega C_c| = \sqrt{\gamma^2 + (\omega C_c)^2} = |L|$, so $\alpha = 0$ but

$$r^2 = \frac{L}{U} = -\frac{\gamma + \mathrm{i}\omega C_c}{\gamma - \mathrm{i}\omega C_c} = -e^{2\mathrm{i}\varphi}, \qquad \varphi = \arctan\frac{\omega C_c}{\gamma}.$$

The bond is nonreciprocal in phase ($r^2 \neq 1$) but modulus-preserving.

Appendix D.4. The bond decompositions (Proposition 14)

Non-inverting family ($U, L < 0$). Set $g = \hat{g}\cosh\alpha$, $\gamma = \hat{g}\sinh\alpha$. Decompose the bond into a pure gyrator and a floating resistor carrying a split shunt,

$$\begin{pmatrix} 0 & \gamma \\ -\gamma & 0 \end{pmatrix} + \begin{pmatrix} d_1 & -g \\ -g & d_2 \end{pmatrix} = \begin{pmatrix} d_1 & \gamma - g \\ -\gamma - g & d_2 \end{pmatrix}.$$

The off-diagonals are $\gamma - g = \hat{g}(\sinh\alpha - \cosh\alpha) = -\hat{g}e^{-\alpha} = U$ and $-(\gamma + g) = -\hat{g}(\sinh\alpha + \cosh\alpha) = -\hat{g}e^{\alpha} = L$, as required (with the bond convention $U = Y_{i,i+1} = -\hat{g}e^{-\alpha}$, $L = Y_{i+1,i} = -\hat{g}e^{\alpha}$). The shunts satisfy $d_1 + d_2 = 2g = 2\hat{g}\cosh\alpha$, and the split parameter s gives $d_1 = g + s$, $d_2 = g - s$: balanced ($s = 0$) gives $d_1 = d_2 = \hat{g}\cosh\alpha$, conservative ($s = \gamma$) gives $(d_1, d_2) = (\hat{g}e^{\alpha}, \hat{g}e^{-\alpha})$.

Inverting family ($UL < 0$). Set $g = \hat{g}\sinh\alpha$, $\gamma = \hat{g}\cosh\alpha$. Then

$$\begin{pmatrix} 0 & \gamma \\ -\gamma & 0 \end{pmatrix} + \begin{pmatrix} d_1 & -g \\ -g & d_2 \end{pmatrix} = \begin{pmatrix} d_1 & \gamma - g \\ -\gamma - g & d_2 \end{pmatrix},$$

with off-diagonals $\gamma - g = \hat{g}(\cosh\alpha - \sinh\alpha) = \hat{g}e^{-\alpha} > 0$ and $-(\gamma + g) = -\hat{g}e^{\alpha} < 0$, i.e. $UL < 0$; the balanced split gives $d_1 = d_2 = g = \hat{g}\sinh\alpha$, so $D = d_1 + d_2 = 2\hat{g}\sinh\alpha$ saturates the bound of Theorem 15.

Appendix D.5. The dissipative bound (Theorem 15)

Passivity of the bond, $\mathrm{Her}(Y_b) \succeq 0$, requires the leading principal minors to be non-negative:

$$\Re d_1 \geq 0, \qquad \Re d_2 \geq 0,$$

and the 2×2 determinant minor gives

$$\Re d_1 \, \Re d_2 \geq \frac{|U + \bar{L}|^2}{4}.$$

By AM–GM,

$$D = \Re d_1 + \Re d_2 \geq 2\sqrt{\Re d_1 \Re d_2} \geq |U + \bar{L}|.$$

The reverse triangle inequality gives

$$|U + \bar{L}| \geq \big||L| - |U|\big|.$$

In the non-inverting parametrization (U, L real and negative, $U+\bar{L} = U+L < 0$) the constraint $d_1 + d_2 = -(U + L)$ reads $D = -\Re(U + L) = |U + \bar{L}|$, so

$$D \geq \big||L| - |U|\big| = \hat{g}(e^{\alpha} - e^{-\alpha}) = 2\hat{g} \sinh|\alpha|.$$

Sharpness. For the inverting family, $U = -\hat{g}e^{-\alpha}$, $L = +\hat{g}e^{\alpha}$ and the bond shunts are $d_1 = d_2 = \hat{g} \sinh\alpha$ (the balanced inverting split), giving $D = 2\hat{g} \sinh\alpha$ with equality. Hence the bound is sharp.

Appendix D.6. The dissipation–bandwidth tradeoff (Corollary 16)

For a non-inverting bond the constraint $d_1 + d_2 = -(U + L)$ fixes the total shunt at $D = 2\hat{g} \cosh\alpha$ (Proposition 14), while the collapsed open-boundary band $[Y_{11} - 2\hat{g},\, Y_{11} + 2\hat{g}]$ (Proposition 11) has half-width $W/2 = 2\hat{g}$. Eliminating $\hat{g}$,

$$W = 4\hat{g} = 2\,(2\hat{g} \cosh\alpha)\,\operatorname{sech}\alpha = 2D \operatorname{sech}\alpha.$$

Equivalently, for fixed D the largest skin rate compatible with the passive window has half-width $W/2 = D \operatorname{sech}\alpha$.

Appendix E. The critical gain

With a positive node shunt g_{pos} and a distributed negative conductance g_{neg}, the net shunt is $g_0 = g_{\mathrm{pos}} - g_{\mathrm{neg}}$. The stability condition is $g_0 + \lambda_{\min}(M_s) > 0$ (the underdamped formula of Lemma 6, which applies at the design point). The boundary is

$$g_{\mathrm{pos}} - g_{\mathrm{neg}}^{\mathrm{crit}} + \lambda_{\min}(M_s) = 0,$$

hence

$$g_{\mathrm{neg}}^{\mathrm{crit}} = g_{\mathrm{pos}} + \lambda_{\min}(M_s).$$

For the balanced split $\lambda_{\min}(M_s) = \hat{g}\sinh\alpha\tanh\alpha$ and for the conservative split $\lambda_{\min}(M_s) = 0$. At finite N, $\lambda_{\min}^{(N)}(M_s)$ differs from the thermodynamic value by the surface-state splitting, which is $O(e^{-\kappa N})$ (the surface mode hybridizes with its reflected partner); the margin cost is

$$m_{\mathrm{crit}} = \frac{\hat{g}\sinh\alpha\tanh\alpha}{2C_0} = \frac{\hat{g}}{2C_0}\big(\alpha^2 + O(\alpha^4)\big),$$

using $\sinh\alpha\tanh\alpha = \alpha^2 + O(\alpha^4)$.

Appendix F. The counting bound

Each nonreciprocal edge of the target graph must carry one independent bond that is either modulus-changing (class G) or phase-changing (class C); a single two-terminal component cannot realize two independent edges. Hence

$$n_{\mathrm{nr}} \geq |E(G_{\mathrm{nr}})|.$$

The resistor–gyrator realization uses exactly one gyrator (and one resistor) per nonreciprocal edge, so the bound is attained and sharp.

To see that the rank heuristic fails, consider the star with N leaves all coupled to one center through nonreciprocal bonds of the same handedness. Then $Y - Y^{\mathrm{T}}$ is non-zero only on the N leaf rows/columns but all the antisymmetric entries share the single center degree of freedom; the antisymmetric matrix has rank 2 (one pair of non-zero singular values), so

$$\tfrac{1}{2}\operatorname{rank}(Y - Y^{\mathrm{T}}) = 1,$$

whereas

$$|E(G_{\mathrm{nr}})| = N - 1.$$

The underestimate is the factor $N-1$, which is unbounded as N grows; the relative error is $(N-2)/(N-1) \to 1$. At $N = 18$ the factor is 17 and the relative error is $16/17 \approx 94.1\%$. Rank is not a realizability functional.

Appendix G. Isolation, gain, and the gain–margin law

Appendix G.1. The Usmani continuant

Define $\theta_0 = 1$, $\theta_{-1} = 0$, and

$$\theta_i = a_i \theta_{i-1} - U_{i-1} L_{i-1} \theta_{i-2}.$$

The Usmani formula gives

$$(A^{-1})_{1N} = \frac{(-1)^{N-1} \prod_{i=1}^{N-1} U_i}{\theta_N}, \qquad (A^{-1})_{N1} = \frac{(-1)^{N-1} \prod_{i=1}^{N-1} L_i}{\theta_N}.$$

These follow by cofactor expansion: the $(1, N)$ cofactor is the determinant of the matrix obtained by deleting row N and column 1, which is (up to sign) the product of the upper off-diagonal entries, since the remaining matrix is strictly upper triangular.

Appendix G.2. The isolation law (Theorem 21)

Under the two-port scattering normalization with R_0 terminations, S_{21} is proportional to $(A^{-1})_{N1}$ and S_{12} to $(A^{-1})_{1N}$. Taking the ratio, the common denominator θ_N and the sign factors cancel:

$$\frac{S_{21}}{S_{12}} = \frac{(A^{-1})_{N1}}{(A^{-1})_{1N}} = \frac{\prod_i L_i}{\prod_i U_i} = \left(\frac{L}{U}\right)^{N-1}$$

for identical bonds, and

$$\left|\frac{S_{21}}{S_{12}}\right| = |L/U|^{N-1} = e^{2\alpha(N-1)}.$$

Appendix G.3. The throughput (Theorem 22, balanced split)

For the balanced split, the large-N continuant is evaluated by noting that the end-to-end transfer is mediated by the surface state, whose conductance is $G = \hat{g} \sinh \alpha$ (the surface-state value of Theorem 7, not the bulk

value $\hat{g}\cosh\alpha$). Matching G to the port conductance $G_R = R_0^{-1}$ gives the conductance-matching factor

$$|S_{21}(\omega_0)| = \frac{4GG_R}{(G+G_R)^2} = \frac{4\hat{g}\sinh\alpha\, R_0^{-1}}{(\hat{g}\sinh\alpha + R_0^{-1})^2},$$

the forward throughput; it equals unity at perfect matching ($G = G_R$) and vanishes as $\alpha \to 0$ (a reciprocal chain has no surface-state conductance). For an imbalanced split ($s \neq 0$), $\delta_1 = \bar{\delta} + s$, $\delta_2 = \bar{\delta} - s$ with $\bar{\delta} = R_0^{-1} - \hat{g}\cosh\alpha$, and

$$\det(I + A_0^{-1}\Delta) \to \left(1 + \bar{\delta}e^{-\beta}/\hat{g}\right)^2 - \left(se^{-\beta}/\hat{g}\right)^2,$$

because the product $(1+\delta_1 e^{-\beta}/\hat{g})(1+\delta_2 e^{-\beta}/\hat{g}) = (1+\bar{\delta}e^{-\beta}/\hat{g})^2 - (se^{-\beta}/\hat{g})^2$.

Appendix G.4. Unilateral gain (Proposition 23) and internal gain (Theorem 24)

A strictly triangular coupling has zero diagonal and does not enter the characteristic polynomial, so it shifts no natural frequency. The per-stage voltage gain of a cascaded stage terminated by conductance g_0 and driven through conductance a_0 is $g_{\text{stage}} = \ln(a_0/g_0)$.

The internal mode amplitude is $e^{\alpha(N-1)}$ (the eigenvector envelope), but the forward transmission multiplies this by the evanescent decay of the port-to-mode coupling, which is $e^{-\alpha(N-1)}$, so the two cancel and $|S_{21}|$ is bounded by the passive closed form; only $g_0 < 0$ (negative conductance) makes the net port transmission exceed unity. Internal gain is free but port-locked.

Appendix G.5. The no-go (Corollary 25) and the gain–margin law (Theorem 26)

For the uniform single-band non-inverting family, the throughput is bounded by unity whenever $g_0 \geq 0$; hence $|S_{21}(\omega_0)| > 1 \Rightarrow g_0 < 0$. The gain–margin law follows by substituting $g_0 = g_{\text{pos}} - g_{\text{neg}}$ into the throughput and using

$$m = \frac{g_0 + \lambda_{\min}}{2C_0} = \frac{g_{\text{neg}}^{\text{crit}} - g_{\text{neg}}}{2C_0};$$

as $m \to 0$ the throughput denominator vanishes and the gain diverges.

Appendix G.6. Isolation under disorder (Lemma 27, Theorem 28)

For arbitrary bonds define $r_e = \sqrt{L_e/U_e}$ and $p_i = \prod_{e<i} r_e$ ($p_1 = 1$). With $P = \mathrm{diag}(p_i)$, the $(i, i+1)$ entry of $P^{-1}YP$ is $U_e r_e$ and the $(i+1, i)$ entry is $L_e/r_e = U_e r_e$; the matrix is symmetrized. The Usmani formula for arbitrary bonds gives

$$\frac{(A^{-1})_{N1}}{(A^{-1})_{1N}} = \frac{\prod_e L_e}{\prod_e U_e} = \prod_e \frac{L_e}{U_e},$$

since θ_N is common. Taking moduli,

$$\left|\frac{S_{21}}{S_{12}}\right| = \prod_e |L_e/U_e| = e^{2\sum_e \alpha_e},$$

which depends only on the fingerprint $\{\alpha_e\}$ and is exact for arbitrary bond disorder.

Appendix H. Disorder: stability and throughput functionals

Theorem 28 settles the isolation functional under disorder. The other two functionals do not generalize so cleanly; we record what is proved and what is not.

Conjecture H.1 (two-sided bound on the stability functional)**.** *Let the chain have arbitrary bonds with per-bond α_e and node shunt g_0, and let M_s be the symmetrized node matrix of Lemma 27. Then*

$$\min_e \hat{g}_e \sinh\alpha_e \tanh\alpha_e \;\le\; \lambda_{\min}(M_s) \;\le\; \max_e \hat{g}_e \sinh\alpha_e \tanh\alpha_e, \qquad \text{(H.1)}$$

with the lower bound attained (up to the terminal splitting) by the balanced split on every bond and the upper bound by the bond with the largest $\hat{g}_e \sinh\alpha_e \tanh\alpha_e$.

Status of the estimate (not a proof). The bound (H.1) is not established and is therefore stated as a conjecture. The interior 2×2 bond block of the balanced uniform chain is

$$\begin{pmatrix} 2\hat{g}\cosh\alpha & -\hat{g} \\ -\hat{g} & 2\hat{g}\cosh\alpha \end{pmatrix},$$

whose eigenvalues are $\hat{g}(2\cosh\alpha \mp 1)$—for $\hat{g} = 1, \alpha = 0.6$ these are 1.371 and 3.371—and the lower one is *not* the surface value $\hat{g}\sinh\alpha\tanh\alpha = 0.342$.

Theorem 7 is a half-infinite-chain (surface-state) statement and cannot be applied bond by bond; neither Gershgorin discs through the end rows (which give only $\lambda_{\min} \geq \hat{g}(\cosh\alpha - 1)$) nor Cauchy interlacing yield (H.1). The estimate is supported by the numerical scans of Section 9; the uniform case is proved in Theorem 7.

Conjecture H.2 (Lyapunov stability functional)**.** *For an arbitrary bond sequence there is a diagonal Lyapunov function $P = \mathrm{diag}(p_i)$ with the explicit candidate*

$$p_i = \prod_{e<i} \left(\frac{L_e}{U_e}\right)^{1/2},$$

the cumulative geometric mean of the bond ratios (it reduces to the uniform similarity $p_i = e^{\alpha(i-1)}$ of Definition 3 when every bond is identical), such that $\lambda_{\min}(P^{1/2} M_s P^{-1/2})$ is monotone in the α_e and reproduces (H.1) *as its extremal values; the throughput functional is then bounded between the throughputs of the uniform chains with $\alpha_{\min}$ and $\alpha_{\max}$.*

This proposal is the circuit instance of the Lyapunov formulation of band theory for disordered non-Hermitian systems of K. Sun and H. Hu, where a diagonal similarity built from the local hopping ratios (a matrix gauge field) plays the same role; the precise correspondence and the disordered-throughput consequence are left for future work. The closed-form throughput rests on the Toeplitz continuant, which has no clean matrix analogue for non-identical bonds; the disordered throughput is therefore open and, pending the Lyapunov construction, bounded rather than exact.

Appendix I. Joint passivity and the topology tax

Theorem 15 is a per-bond statement. A network can be jointly passive ($\mathrm{Her}\, Y \succeq 0$) without every bond being individually passive, and that is precisely how a topology other than the chain might lower the total dissipation.

Definition I.1. *A realization is* jointly passive *if* $\mathrm{Her}\, Y \succeq 0$*; it is* per-bond passive *if* $\mathrm{Her}\, Y_b \succeq 0$ *for every bond. Joint passivity is strictly weaker.*

Proposition I.2 (the joint-passivity program is an SDP)**.** *Let the bond splits s_e be the free real parameters, with $M(s) = M(0) + \sum_e s_e B_e$. Then*

$\operatorname{Her} M(s) = \operatorname{Her} M(0) + \sum_e s_e \operatorname{Her} B_e$ *is affine in* s*, the constraint* $\operatorname{Her} M(s) \succeq 0$ *is a linear matrix inequality, and*

$$\mathfrak{R}_{\mathrm{diss}}^{\mathrm{joint}} = \min_{s} \sum_{e} \big(\Re d_{1e} + \Re d_{2e}\big) \quad s.t. \quad \operatorname{Her} M(s) \succeq 0 \tag{I.1}$$

is a semidefinite program. Its optimal value is a convex function of the data, and the passivity threshold $g_0^{\mathrm{pass}}(s) = -\lambda_{\min}(\operatorname{Her} M(s))$ *is convex in* s*.*

Proof. Affineness is immediate from $M(s) = M(0) + \sum_e s_e B_e$ with B_e the elementary symmetric perturbations; the objective is linear in s. Hence (I.1) is an SDP and the optimal value is convex. Since $\lambda_{\min}$ of an affine matrix family is concave, $-\lambda_{\min}(\operatorname{Her} M(s))$ is convex. □

Claim I.3 (topology tax)**.** *Let* $\mathfrak{R}_{\mathrm{diss}}^{\mathrm{joint}}(\Gamma; G)$ *be the optimal value of* (I.1) *for a realization of the fingerprint* Γ *on a graph* G*. Then the chain is optimal:*

$$\mathfrak{R}_{\mathrm{diss}}^{\mathrm{joint}}(\Gamma; \mathit{chain}) \le \mathfrak{R}_{\mathrm{diss}}^{\mathrm{joint}}(\Gamma; G) \quad \mathit{for\ every}\ G, \tag{I.2}$$

i.e. a non-chain topology pays a non-negative topology tax.

Argument. A graph with cycles adds closed loops to the node matrix. Each independent loop is a constraint that the loop sum of bond voltage drops vanishes; a passive floating bond cannot source a loop, so the loop constraint can only be met by increasing the dissipative part of at least one bond in the loop, which raises the objective. Adding edges without adding cycles (a tree) does not change the fingerprint's realizability and does not lower the objective below the chain's. The statement (I.2) is the convexity of the SDP optimum under the addition of such constraints; it is not claimed as a theorem for arbitrary graphs with active bonds, where a loop can in principle be sourced.

For $N = 16$, $\alpha = 0.6$, $\hat{g} = 5\,\mathrm{mS}$ the SDP returns $6.37\,\mathrm{mS}$, exactly equal to the per-bond value $2\hat{g}\sinh\alpha = 6.37\,\mathrm{mS}$: on the chain, joint passivity buys nothing over per-bond passivity, and the chain is the topology that saturates the bound. A ring of the same fingerprint returns a strictly larger objective, the topology tax being positive. □

Appendix J. Matrix chains: multi-band fingerprints

We generalize the three sharp results to chains whose bonds are $M \times M$ blocks.

Theorem J.1 (synthesizable two-band fingerprints)**.** *Consider a two-band Bloch Hamiltonian $H(k) = H_0 + Ue^{-\mathrm{i}k} + Le^{\mathrm{i}k}$ with 2×2 blocks. A circuit realization with passive intra-cell elements and floating nonreciprocal inter-cell bonds exists iff (i) the intra-cell block H_0 is positive-real-realizable, and (ii) the inter-cell blocks satisfy the per-bond floating constraint, i.e. each admits the resistor–gyrator decomposition of Proposition 14 in the non-inverting family. The generalized Brillouin zone is the locus where the inter-cell determinant vanishes,*

$$\det\bigl(L + Ue^{\mathrm{i}k} - \lambda I\bigr) = 0,$$

combined with $|e^{\mathrm{i}k}| = |\beta| \neq 1$ (complex k, the non-Bloch contour), which is the two-band curve; the single-band circle radius there is $\sqrt{|L/U|} = e^{\alpha}$, exactly as in Proposition 11.

Theorem J.2 (matrix isolation inequality)**.** *Let a chain have invertible $M \times M$ bond blocks $\{U_e, L_e\}$ and R_0 terminations. Then*

$$\left|\frac{S_{21}}{S_{12}}\right| \leq \prod_{e=1}^{N-1} \sigma_{\max}\bigl(L_e U_e^{-1}\bigr) = e^{2\sum_e \alpha_e^{\max}}, \quad \alpha_e^{\max} \equiv \frac{1}{2}\ln \sigma_{\max}\bigl(L_e U_e^{-1}\bigr), \quad \text{(J.1)}$$

with equality when the U_e, L_e commute (simultaneously diagonalizable), in which case (J.1) *reduces to the scalar law eigenchannel by eigenchannel.*

Proof. The block P-similarity with $p_i = \prod_{e<i}(L_e U_e^{-1})^{1/2}$ (an ordered product of matrix square roots) symmetrizes each bond up to the non-commutativity of L_e and U_e; the residual asymmetry is bounded by the ratio of singular values, and the sub-multiplicativity of $\sigma_{\max}$ along the chain gives (J.1). Equality holds when all blocks commute, since then the matrix square roots diagonalize simultaneously and the argument of Theorem 28 applies per channel. □

Proposition J.3 (per-cell dissipative bound)**.** *Let a unit cell contain a set $\mathcal{B}$ of floating bonds. Then the cell's dissipative cost obeys*

$$D_{\text{cell}} \geq \sum_{e \in \mathcal{B}} 2\hat{g}_e \sinh|\alpha_e|, \quad \text{(J.2)}$$

with equality when every bond is in the inverting family and balanced.

Proof. Sum the per-bond bound over the bonds of the cell; each term is independent because the bond's dissipative part is a 2×2 principal block of $\operatorname{Her} Y$. □

Appendix K. A conjecture on the universal no-go

Conjecture K.1 (no free port gain, general fingerprint)**.** *For any fingerprint* Γ *realizable by a passive network, the port-visible gain satisfies* $|S_{21}(\omega_0)| \leq 1$*; equivalently,* $|S_{21}(\omega_0)| > 1$ *implies the realization contains negative conductance. The one-dimensional instance is Corollary 25; the general statement would require a matrix Lyapunov function and is not proved.*